

Effect of La Doping on Microstructure and Critical Current Density of MgB_2

Chandra Shekhar^a, Rajiv Giri^a, R S Tiwari^a, D S Rana^b, S K Malik^b and O N Srivastava^{a}*

^a Department of Physics, Banaras Hindu University, Varanasi 221005, India

^b Tata Institute of Fundamental Research, Mumbai-400005, India

Abstract

In the present study, La-doped MgB_2 superconductors with different doping level ($\text{Mg}_{1-x}\text{La}_x\text{B}_2$; $x=0.00, 0.01, 0.03$ & 0.05) have been synthesized by solid-state reaction route at ambient pressure. Effect of La doping have been investigated in relation to microstructural characteristics and superconducting properties, particularly intragrain critical current density (J_c). The microstructural characteristics of the as synthesized $\text{Mg}(\text{La})\text{B}_2$ compounds were studied employing transmission electron microscopic (TEM) technique. The TEM investigations reveal inclusion of LaB_6 nanoparticles within the MgB_2 grains which provide effective flux pinning centres. The evaluation of intragrain J_c through magnetic measurements on the fine powdered version of the as synthesized samples reveal that J_c of the samples change significantly with the doping level. The optimum result on J_c is obtained for $\text{Mg}_{0.97}\text{La}_{0.03}\text{B}_2$ at 5K, the J_c reaches $\sim 1.4 \times 10^7 \text{ A/cm}^2$ in self field, $\sim 2.1 \times 10^6 \text{ A/cm}^2$ at 1T, $\sim 2.5 \times 10^5 \text{ A/cm}^2$ at 2.5T and $\sim 1.8 \times 10^4 \text{ A/cm}^2$ at 4.5T. The highest value of intragrain J_c in $\text{Mg}_{0.97}\text{La}_{0.03}\text{B}_2$ superconductor has been attributed to the inclusion of LaB_6 nanoparticles which are capable of providing effective flux pinning centres.

PACS : 74.70Ad; 74.25Sv; 74.62Dh; 74.25Ha

Key words : superconductor, nanoparticle, intragrain J_c

*Corresponding author

E-mail: hepons@yahoo.com, girirajiv_bhu@yahoo.com

Introduction

The discovery of superconductivity at 40K in MgB_2 by Nagamatsu et al. [1] has generated a great deal of excitement in both fundamental and practical investigations of this material. One advantage of MgB_2 is in regard to its applications at comparatively higher temperatures (20-30K) region, where the conventional superconductors can not operate. Also, the progress in cryogen free cooling technique at temperature region of 20-30K will promote the development and application of MgB_2 . Another important aspect in MgB_2 bulk material is that supercurrent flow is largely unhindered by grain boundaries (GBs) [2,3], thus providing a high feasibility of scaling up the material to form bulk shapes like wire and tapes. For widespread applications of MgB_2 high value of critical current density in higher magnetic field is required and hence need of adequate flux pinning centres is evident. The effective flux pinning is known to occur when core of fluxoids find higher density normal materials to sit on. Strong pinning centres prevent flux melting and the consequent creep. If local structural perturbations are strong and these are isolated, they can act as effective flux pinning centres provided that their sizes are compatible with the coherence length ($\sim 6\text{nm}$). Unfortunately, the bulk materials prepared at ambient pressure always show lower J_c value due to poor grain connectivity, low density and poor flux pinning [4,5]. It is found that most efficient techniques used to fabricate high quality MgB_2 samples are hot-isostatic pressing and uniaxial hot pressing at high pressures [6,7]. Also, proton and neutron irradiation are applied to enhance J_c properties in MgB_2 superconductors [8,9]. However, these techniques are not suitable for the preparation of MgB_2 wire and tapes because of their complicated nature and the practical difficulty in the use of very large vessels and dyes in case of high temperature and high pressure. On the other hand, it is reported that chemical doping is effective to increase J_c in high- T_c cuprates superconductors [10]. Similar techniques have been also utilized for the MgB_2 materials. Recently Dou et al. [11] and Matsumoto et al. [12] have synthesized MgB_2 superconductor in bulk form at ambient pressure through doping of SiC and SiO_2 & SiC respectively. They have reported enhancement of flux pinning properties due to nano inclusion of SiC (10-100 nm) into MgB_2 grains. Many groups have been trying to improve the J_c by chemical doping. At 20K, pure MgB_2 generally has a intragrain J_c of about 10^4 A/cm^2 under 1T and irreversible field (H_{ir}) is about 4T [7, 13,14]. It may be pointed out that the estimation of $J_c \sim 10^4 \text{ A/cm}^2$ (at 1T and 20K) is for undoped samples devoid of any flux pinning centers. However, when doping is done to produce flux pinning centers, this estimate generally become $\sim 10^5 \text{ A/cm}^2$ (at 1T and 20K) [15-18]. The Ti doping (few to ~ 10

atomic%) in MgB_2 has been known to enhance intragrain J_c (evaluated through magnetization measurement and using Bean's formula) values upto 10^5 A/cm^2 under 1T and H_{irr} near 5T at 20K with small T_c reduction [15, 16]. Shu-Fang Wang et al. [17] have reported that J_c increases up to $5 \times 10^5 \text{ A/cm}^2$ at 5K and in self field for Cd doped MgB_2 . Rui et al. have reported enhancement of J_c by adding nano-alumina (10-50nm) into MgB_2 [18]. It should be pointed out that the above authors have used Bean's formula to estimate intragrain J_c . Recently doping of Al, Fe, Au, Pb into MgB_2 have been reported for improvement of flux pinning centres and consequently enhancement in intragrain J_c values [19-22]. To date, two important factors of low density and poor flux pinning are main obstacles to obtain high J_c value in MgB_2 superconductor. Therefore, it is necessary to carry out further research by addition and doping of suitable elements into MgB_2 to understand the mechanism of the flux pinning in MgB_2 and eventually realize the widespread applications of MgB_2 . It is known that microstructural features affect crucially the critical current density of superconducting materials. Therefore, in order to explore the microstructural characteristics and its possible correlation with superconducting properties, particularly J_c , in the present paper, we have studied structural, microstructural characteristics of the as synthesized $\text{Mg}_{1-x}\text{La}_x\text{B}_2$ ($0.00 \leq x \leq 0.1$) samples employing transmission electron microscopic (TEM) technique. TEM investigation reveals nanoparticle LaB_6 inclusions within the MgB_2 grains.

The intragrain critical current density (J_c) evaluated through magnetic measurement for sample with various compositions have been found to vary significantly e.g. J_c of $\text{Mg}_{0.97}\text{La}_{0.3}\text{B}_2$ sample is $\sim 2.1 \times 10^6 \text{ A/cm}^2$ and for $\text{Mg}_{0.99}\text{La}_{0.01}\text{B}_2$ sample, it is $\sim 6.5 \times 10^5 \text{ A/cm}^2$ at 5K and 1T. A correlation between intragrain J_c and details of the microstructure has been shown to exist. The $\text{Mg}_{0.97}\text{La}_{0.3}\text{B}_2$ sample which possesses the highest intragrain $J_c \sim 1.4 \times 10^7 \text{ A/cm}^2$ in self field at 5K exhibits LaB_6 nanoparticle in the MgB_2 grains.

Experimental details

The synthesis of La doped MgB_2 with nominal composition of $\text{Mg}_{1-x}\text{La}_x\text{B}_2$ ($0.00 \leq x \leq 0.1$) has been carried out by solid state reaction method at ambient pressure by employing a special encapsulation technique developed in our laboratory. The powders [Mg (99.9%), La (99%) and B (99%)] were fully mixed and were cold pressed (3.0 tons/inch^2) into small rectangular pellets ($10 \times 5 \times 1 \text{ mm}^3$). Then the pellets of $\text{Mg}(\text{La})\text{B}_2$ were encapsulated in a Mg metal cover to circumvent the formation of MgO during sintering

process. The pellet configuration was put on a Ta boat and sintered in flowing Ar atmosphere in a tube furnace at 600°C for 1h, at 800°C for 1h and at 900°C for 2h. The pellet was cooled to room temperature at the rate of 100°C/h. The pellet was taken out and encapsulating Mg cover was removed. The details of the synthesis were similar as described in our earlier publication [23]. All the samples in the present investigation were subjected to gross structural characterization by X-ray diffraction technique (XRD, Philips PW-1710 CuK α), electrical transport characterization by four-probe technique (Keithley resistivity Hall set-up), the microstructural characterization by transmission electron microscope (Philips EM-CM-12) and elemental composition was determined by energy dispersive X-ray analysis (EDAX, Oxford-ENCA). The magnetization measurements have been carried out at Tata Institute of Fundamental Research (Mumbai, India) over a temperature range of 5-40K employing a physical property measurement system (PPMS, Quantum Design). Intragrain J_c (magnetic J_c) was calculated from the height ' ΔM ' of the magnetization loop (M-H) using Bean's critical state model [24]. It should be pointed out that Bean's formula leads to the optimum estimate of intragrain J_c for superconductors having weakly coupled grains. It is not quite appropriate for bulk MgB $_2$ superconductors because of strong grain coupling in this material. The magnetization measurements have been carried out on fine ground powders of the as synthesized samples. In the fine powder form, strong coupling is non-existent, the intragrain critical current density can be estimated employing Bean's formula and using average size of the powder particles. Usually, the particles after grinding of samples may not correspond to singular grains but are as estimated through SEM small agglomerates of nearly spherical shape ($\sim 5 \mu\text{m}$) covering only few grains. The intragrain J_c , therefore, can be estimated by the following formula :

$$J_c = \frac{30\Delta M}{< d >}$$

Where ' ΔM ' is change in magnetization with increasing and decreasing field (in emu/cm 3) and ' d ' is average particle size (in cm).

Results and discussion

The dc magnetic susceptibility (χ) of Mg $_{1-x}$ La $_x$ B $_2$ (with $x=0.01, 0.03, 0.05$) superconducting samples are shown in Fig. 1 for 50 Oe field as a function of temperature. The χ -T curve shows diamagnetic onset transition temperature for Mg $_{0.99}$ La $_{0.01}$ B $_2$,

$\text{Mg}_{0.97}\text{La}_{0.03}\text{B}_2$ and $\text{Mg}_{0.95}\text{La}_{0.05}\text{B}_2$ samples to be 40K, 39K and 37K respectively. The central aim of the present investigation is to explore the flux pinning centres originating as a result of doping. We first describe various microstructural features induced by different doping levels of La at Mg site of MgB_2 compound. Thereafter, evaluation of critical current density through magnetic hysteresis loop and correlation between microstructural features and intragrain J_c will be described and discussed. In order to investigate microstructural features of La doped MgB_2 , we carried out extensive studies of nature of grain boundaries (GBs) and inclusion of secondary particles by employing the technique of TEM, which is considered to be the viable technique for such studies.

Fig. 2(a) shows a representative transmission electron micrograph for $\text{Mg}_{0.99}\text{La}_{0.01}\text{B}_2$ compound. The dominant feature resulting from this doping is the occurrence of LaB_6 nanoparticles which are found to be invariably present. The selected area diffraction pattern corresponding to TEM micrograph is shown in Fig. 2(b). The slight splitting of diffraction spots reveals the presence of low angle grain boundaries in $\text{Mg}_{0.99}\text{La}_{0.01}\text{B}_2$ compound.

Fig. 2(c) represents the TEM micrograph of $\text{Mg}_{0.97}\text{La}_{0.03}\text{B}_2$ compound. The dominant and specific microstructural feature for this compound is the presence of high density of LaB_6 nanoparticles within MgB_2 grains. The size of these nanoparticles lies in the range of 5-15nm. Among these nano inclusions, those which are compatible with coherence length of MgB_2 (~6nm) may work as effective flux pinning centres. The SAD pattern corresponding to TEM micrograph [shown in Fig. 2(d)] reveals the spotty ring pattern. These diffraction rings, which correspond to LaB_6 and MgB_2 , depict the inclusion of LaB_6 nanoparticle in MgB_2 grains.

The TEM micrograph for $\text{Mg}_{0.95}\text{La}_{0.05}\text{B}_2$ revealing the presence of LaB_6 nanoparticles (20-35 nm) is discernible from the micrograph Fig. 2(e). It is interesting to note that the size of LaB_6 nanoparticle in this compound is bigger than those of the $\text{Mg}_{0.97}\text{La}_{0.03}\text{B}_2$ compound [as shown in Fig. 2(c)] and has low density of nanoparticles. The SAD pattern corresponding to TEM micrograph [shown in fig. 2(e)] reveals hexagonal arrangement of diffraction spots of MgB_2 along with square diffraction spots of cubic LaB_6 . The diffraction spots of the SAD pattern of $\text{Mg}_{0.95}\text{La}_{0.05}\text{B}_2$ [Fig. 2(f)] have been indexed. These results clearly show that with different doping concentration of La at Mg site of MgB_2 their microstructural features manifested by the occurrence of LaB_6 nanoparticles vary significantly.

The magnetization measurements as a function of magnetic fields have been carried out at temperature 5K, 10K, 20K and 30K, for each samples in the powder form. It may

further be pointed out that several workers have employed Bean's formula for the undoped and doped MgB_2 samples [7, 21, 25, 26].

Keeping the above in view, in the following we will proceed to describe the estimation of J_c (intragrain) for the present $\text{Mg}_{1-x}\text{La}_x\text{B}_2$ samples as obtained on powder form. The intragrain J_c as function of magnetic field at temperatures of 5K, 10K, 20K and 30K for MgB_2 , $\text{Mg}_{0.99}\text{La}_{0.01}\text{B}_2$, $\text{Mg}_{0.97}\text{La}_{0.03}\text{B}_2$ and $\text{Mg}_{0.95}\text{La}_{0.05}\text{B}_2$ are shown in Fig. 3(a), 3(b), 3(c) and 3(d) respectively. It is clear from J_c vs H curves, the intragrain J_c of $\text{Mg}_{0.97}\text{La}_{0.03}\text{B}_2$ compound attains the highest value among all the compounds for all temperature and the whole field region upto 5T. This compound contains high density of LaB_6 nanoparticles (~5-15 nm) inclusion into MgB_2 matrix. As for example at 5K, the J_c of $\text{Mg}_{0.97}\text{La}_{0.03}\text{B}_2$ compound is $\sim 1.4 \times 10^7 \text{ A/cm}^2$ in self field and $\sim 2.1 \times 10^6 \text{ A/cm}^2$ at 1T, $\sim 2.5 \times 10^5 \text{ A/cm}^2$ at 2.5T and $\sim 1.8 \times 10^4 \text{ A/cm}^2$ at 4.5T. For $\text{Mg}_{0.99}\text{La}_{0.01}\text{B}_2$ compound, which is nearly without inclusion of LaB_6 nanoparticles, J_c values at 5K are $\sim 6.0 \times 10^6 \text{ A/cm}^2$ in self field, $\sim 6.5 \times 10^5 \text{ A/cm}^2$ at 1T, $\sim 8.6 \times 10^4 \text{ A/cm}^2$ at 2.5T and $\sim 5.6 \times 10^3 \text{ A/cm}^2$ at 4.5T. The intragrain J_c values for $\text{Mg}_{0.95}\text{La}_{0.05}\text{B}_2$ compound, having low density of larger LaB_6 nanoparticles in comparison to $\text{Mg}_{0.97}\text{La}_{0.03}\text{B}_2$ compound, are also lower than $\text{Mg}_{0.97}\text{La}_{0.03}\text{B}_2$. The J_c value for $\text{Mg}_{0.95}\text{La}_{0.05}\text{B}_2$ compound achieves the value of $\sim 1.2 \times 10^6 \text{ A/cm}^2$, $\sim 2.6 \times 10^5 \text{ A/cm}^2$, $\sim 4.4 \times 10^4 \text{ A/cm}^2$ and $\sim 1.0 \times 10^4 \text{ A/cm}^2$ at 5K in self field, 1T, 2.5T and 4.5T respectively. Similar variations of J_c with magnetic field were also observed at temperatures 10K, 20K and 30K. Table-1 brings out the comparison of intragrain J_c values for the undoped and optimally doped MgB_2 samples in the self field and various magnetic fields. As can be seen from this table, J_c s for La doped MgB_2 sample ($\text{Mg}_{0.97}\text{La}_{0.03}\text{B}_2$) is higher than undoped version for all fields.

These results are first of their type for MgB_2 superconductors. All the J_c data reported here by us are much higher than the best results reported so far for MgB_2 bulk materials including those prepared under high pressure (the typical value of J_c is $\sim 2 \times 10^4 \text{ A/cm}^2$ at 20K and 1T) [7], Ti doped MgB_2 (the typical value of J_c is $\sim 2 \times 10^6 \text{ A/cm}^2$ at 5K and in self field) [15], Cd doped MgB_2 (the typical value of J_c at 5K and in self field is $\sim 5 \times 10^5 \text{ A/cm}^2$) [17] and Au coated MgB_2 thin film (the typical value of J_c is $\sim 1.22 \times 10^7 \text{ A/cm}^2$ at 5K and in self field [21]).

It may be noticed from the J_c vs H behavior of La doped MgB_2 samples that J_c decreases slowly with increasing magnetic field. This manifests the presence of effective flux pinning centres in La doped compounds. As revealed by microstructural analyses the nanoparticles of LaB_6 (which are comparable in size to the coherence length) may be

responsible for high intragrain J_c values in the whole range of temperature and magnetic field investigated in the present work.

Conclusion

In conclusion, we have successfully synthesized La doped MgB_2 compounds by solid-state reaction at ambient pressure employing a special encapsulation technique. In the present investigation exploration of microstructural features induced by doping of La at Mg site of MgB_2 compound and its correlation with intragrain critical density (J_c) have been carried out. The highest J_c value at 5K ($\sim 1.4 \times 10^7$ A/cm² in self field, $\sim 2.1 \times 10^6$ A/cm², $\sim 2.5 \times 10^5$ A/cm² and $\sim 1.8 \times 10^4$ A/cm² at field of 1 T, 2.5T and 4.5T respectively), has been obtained for $Mg_{0.97}La_{0.03}B_2$ compound. This enhancement of J_c for specific La doping ($Mg_{0.97}La_{0.03}B_2$) has been found to result due to high density of LaB_6 nanoparticle inclusions in MgB_2 grains which provide effective flux pinning centres.

Acknowledgement

The authors are grateful to Prof. A.R. Verma, Prof. C.N.R. Rao, Prof. A.V. Narlikar and Prof. T.V.Ramakrishnan for fruitful discussions. We put our sincere thanks to Dr. N.P. Lalla for his kind help in EDAX measurements. Financial supports from UGC and CSIR are gratefully acknowledged.

References

- [1] Nagamatsu J, Norimasa N, Muranaka T, Zenitani Y and Akimitsu J 2001 Nature **410** 63
- [2] Larbalestier D C et al. 2001 Nature **410** 186
- [3] Bugoslavsky Y, Perkins G K, Qi X, Cohen L F and Caplin A D 2001 Nature **410** 563
- [4] Finnemore D K, Ostenson J E, Bud'ko S L, Lapertot G and Canfield P C 2001 Phys. Rev. Lett. **86** 2420
- [5] Kambara M, Babu N H, Sadki E S, Cooper J R, Minami H, Cardwell D A, Campbell A M and Inoue I H 2001 Supercond. Sci. Technol. **14** L5
- [6] Serquis A, Liao X Z, Zhu Y T, Coulter J Y, Huang J Y, Willis J O, Peterson D E, Mueller F M, Moreno N O, Thompson J D, Nesterenko V F and Indrakanti S S 2002 J. Appl. Lett. **92** 351
- [7] Takano Y, Takeya H, Fujii H, Kumakura H, Hatano T Togano K, Kito H and Ihara H 2001 Appl. Phys. Lett. **78** 2914
- [8] Bugoslavsky Y, Cohen L F, Perkins G K, Polichetti M, Tate T J, William R and Caplin D 2001 Nature **411** 561
- [9] Eisterer M, Zehetmayer M, Tönies S, Weber H W, Kambara M, Babu N H, Cardwell D A and Greenwood L R 2002 Supercond. Sci. Technol. **15** L9
- [10] Giri Rajiv, Singh H K, Tiwari R S, and Srivastava O N 2001 Bull. Mater.Sci. **24** 523
- [11] Dou S X, Soltanian S, Horvat J, Wang X L, Zhou S H, Ionescu M, Liu H K, Munroe P, and Tomsic M 2002 Appl. Phys. Lett. **81** 3419
- [12] Matsumoto A, Kumakura H, Kitaguchi H and Hatakeyama H 2003 Supercond. Sci. Technol. **16** 926
- [13] Canfield P C, Bud'ko S L and Finnemore D K 2003 Physica C **385** 1
- [14] Jin S, Mavoori H, Bower C and Dover R B van 2001 Nature **411** 563
- [15] Zhao Y, Cheng C H, Feng Y, Machi T, Huang D X, Zhou L, Koshizuka N and Murakami M 2003 Physica C **386** 581
- [16] Anderson Jr N E, Straszheim W E, Bud'ko S L, Canfield P C, Finnemore D K and Suplinskas R J 2003 Physica C **390** 11
- [17] Shu-fang Wang et al. 2004 J. Superconductivity :Incorporating novel Magnetism **17** (3) 397

- [18] Rui X F, Chen J, Chen X, Guo W and Zhang H 2004 Physica C, **412** 312
- [19] Berenov A, Serquis A, Liao X Z, Zhu Y T, Peterson D E, Bugoslavsky Y, Yates K A, Blamire M G, Cohen L F, Mac J L and Driscoll M 2004 Supercond. Sci. Technol. **17** 1093
- [20] Gao Y D, Ding J, Chen Q, Rao G V S and Chowdari B V R 2004 Acta Materialia **52** 1543
- [21] Choi E M, Lee H S, Kim H, Lee S I, Kim H J and Kang W N 2004 Appl. Phys. Lett. **84** 82
- [22] Gu D W, Cai Y M, Yau J K F, Cui Y G, Wu T, Yuan G Q, Shen L J and Jin X 2003 Physica C **386** 643
- [23] Shekhar C, Giri R, Tiwari R S and Srivastava O N 2004 Cryst. Res. Technol. **39** 718
- [24] Bean C P 1964 Rev. Mod. Phys. **36** 31
- [25] Joshi Amish G, Pillai C G S, Raj P, Malik S K 2001 Solid State Communication **118** 445
- [26] Serquis A, Liao X Z, Civale L, Zhu Y T, Coulter J Y, Peterson D E and Mueller F M 2003 IEEE trans. Appl. Supercond. **13** 3068

Figure Captions

- Fig. 1: Temperature dependence of dc magnetic susceptibility for $\text{Mg}_{1-x}\text{La}_x\text{B}_2$ (with $x=0.01, 0.03, 0.05$)
- Fig. 2(a): A representative TEM micrograph of $\text{Mg}_{0.99}\text{La}_{0.01}\text{B}_2$ compound. Presence of low density of LaB_6 nanoparticles (some of which are marked by \rightarrow) may be noticed.
- Fig. 2(b): Selected area diffraction pattern from the region shown in Fig. 2(a). The splitting of spots is due to the presence of low angle grain boundaries.
- Fig. 2(c): TEM micrograph corresponding to $\text{Mg}_{0.97}\text{La}_{0.03}\text{B}_2$ compound, showing the high density of LaB_6 nanoparticles (~ 5 to ~ 15 nm) within the MgB_2 grains.
- Fig. 2(d): Selected area diffraction pattern corresponding to micrograph Fig. 2(c) depicts spotty ring pattern which correspond to MgB_2 and LaB_6 .
- Fig. 2(e): TEM micrograph corresponding to $\text{Mg}_{0.95}\text{La}_{0.05}\text{B}_2$ compound revealing LaB_6 nanoparticles which are bigger in size (~ 20 to ~ 35 nm) than those found for $\text{Mg}_{0.97}\text{La}_{0.03}\text{B}_2$.
- Fig. 2(f): Selected area diffraction pattern corresponding to micrograph Fig. 2(e) reveals hexagonal arrangement of diffraction spots of MgB_2 along with square diffraction spots of LaB_6 which has cubic lattice (marked by \rightarrow).
- Fig. 3: Intragrain critical current density (estimated on fine powder version of the samples) as a function of applied magnetic field at a temperature of 5K, 10K, 20K and 30K for (a) MgB_2 (b) $\text{Mg}_{0.99}\text{La}_{0.01}\text{B}_2$, (c) $\text{Mg}_{0.97}\text{La}_{0.03}\text{B}_2$, (d) $\text{Mg}_{0.95}\text{La}_{0.05}\text{B}_2$, superconductors. Highest critical current density for the $\text{Mg}_{0.97}\text{La}_{0.03}\text{B}_2$ compound may be noticed.

Table-1

Comparision of intragrain J_c (A/cm^2) at 5K for undoped MgB_2 and optimally doped $Mg_{0.97}La_{0.03}B_2$

Compositions	Intragrain J_c (A/cm^2) at 5K			
	Self field	1T	2.5T	4.5T
Undoped MgB_2	3.0×10^5	9.4×10^4	1.8×10^4	8.7×10^2
$Mg_{0.97}La_{0.03}B_2$ (optimally doped)	1.4×10^7	2.1×10^6	2.5×10^5	1.8×10^4

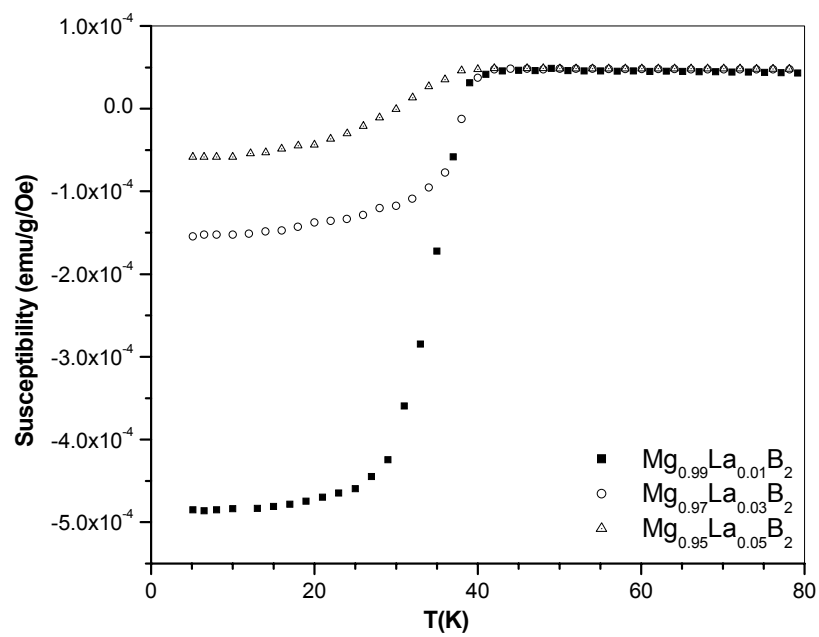


Fig. 1

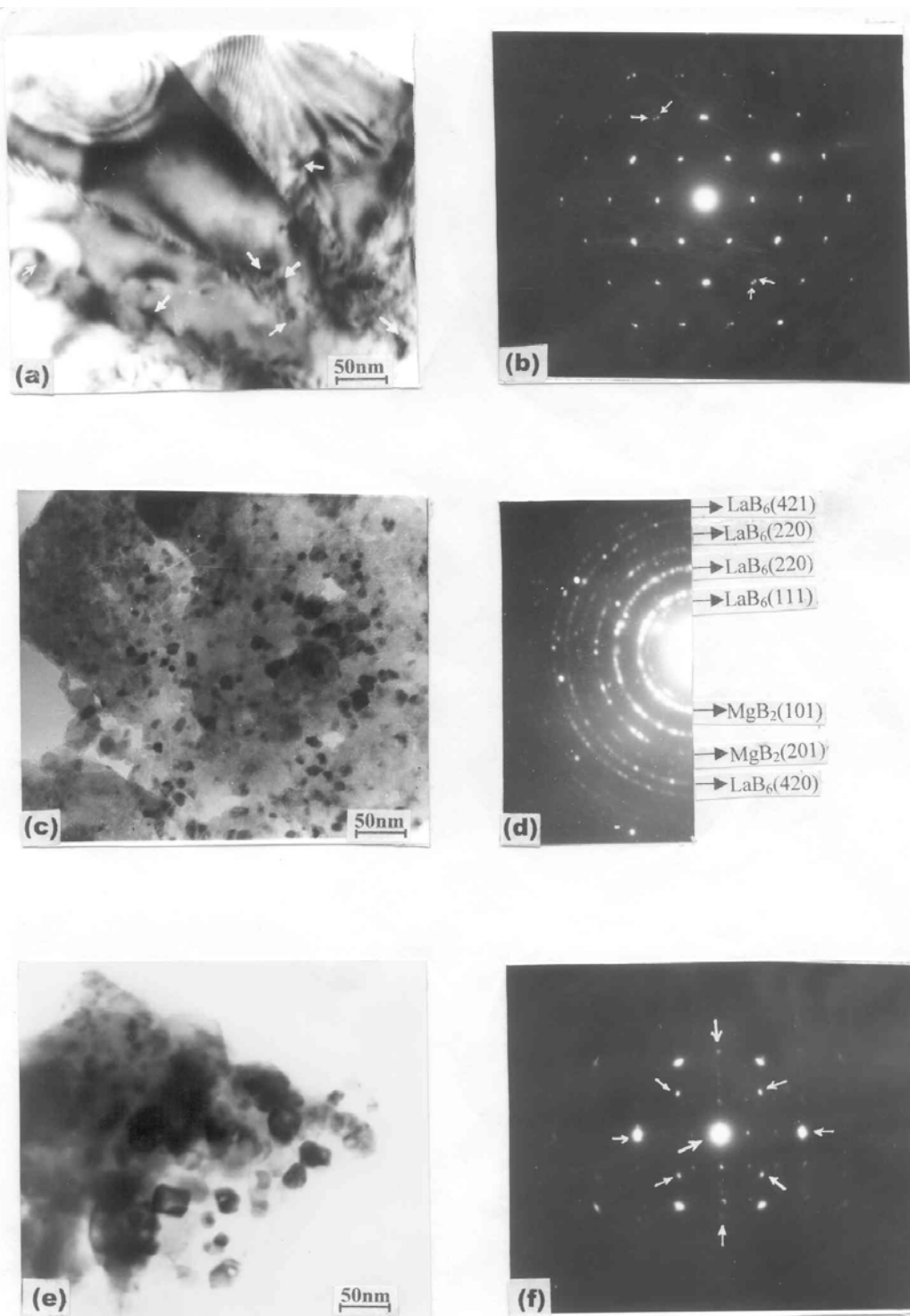


Fig.2

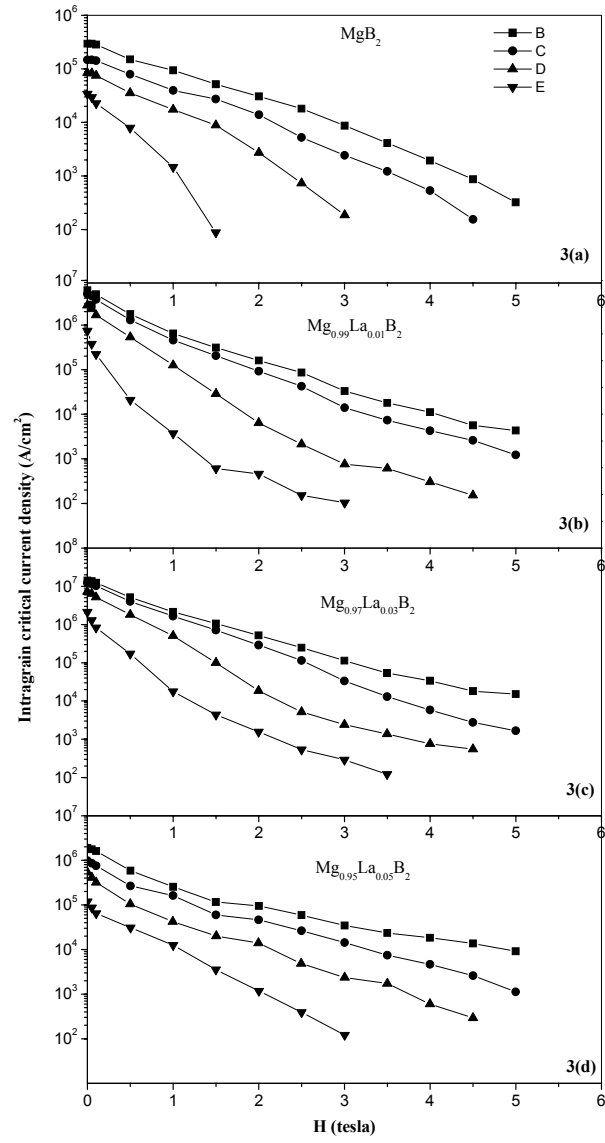


Fig. 3